ChemComm

Accepted Manuscript

This article can be cited before page numbers have been issued, to do this please use: K. Herasymchuk, J. J. Miller, G. MacNeil, A. Sergeenko, D. McKearney, S. Goeb, M. Salle, D. B. Leznoff and T. Storr, *Chem. Commun.*, 2019, DOI: 10.1039/C9CC02320H.

This is an Accepted Manuscript, which has been through the Royal Society of Chemistry peer review process and has been accepted for publication.

Accepted Manuscripts are published online shortly after acceptance, before technical editing, formatting and proof reading. Using this free service, authors can make their results available to the community, in citable form, before we publish the edited article. We will replace this Accepted Manuscript with the edited and formatted Advance Article as soon as it is available.

You can find more information about Accepted Manuscripts in the author guidelines.

Please note that technical editing may introduce minor changes to the text and/or graphics, which may alter content. The journal's standard Terms & Conditions and the ethical guidelines, outlined in our author and reviewer resource centre, still apply. In no event shall the Royal Society of Chemistry be held responsible for any errors or omissions in this Accepted Manuscript or any consequences arising from the use of any information it contains.

ROYAL SOCIETY OF CHEMISTRY

rsc.li/chemcomm

ROYAL SOCIETY OF CHEMISTRY View Article Online
DOI: 10.1039/C9CC02320H

Journal Name

COMMUNICATION

Coordination-driven assembly of a supramolecular square and oxidation to a tetra-ligand radical species

Khrystyna Herasymchuk,[a] Jessica J. Miller,[a] Gregory A. MacNeil,[a] Ania S. Sergeenko,[a] Declan McKearney,[a] Sébastien Goeb,[b] Marc Sallé,[b] Daniel B. Leznoff[a] and Tim Storr*[a]

Received 00th January 20xx,
Accepted 00th January 20xx

DOI: 10.1039/x0xx00000x

www.rsc.org/

The design and synthesis of a supramolecular square was achieved by coordination-driven assembly of redox-active nickel(II) salen linkers and (ethylenediamine)palladium(II) nodes. The tetrameric geometry of the supramolecular structure was confirmed via MS, NMR, and electrochemical experiments. While oxidation of the monomeric metalloligand Schiff-base affords a Ni(III) species, oxidation of the coordination-driven assembly results in ligand radical formation.

Coordination-driven self-assembly has gained significant attention in the field of supramolecular chemistry, providing access to a myriad of structures such as two-dimensional polygons and/or three-dimensional cages, bowls and prisms. These assemblies have been used for applications such as catalysis, guest encapsulation, sensing, drug delivery, nanomaterials and light harvesting.[1] In addition, the dynamic self-assembly of nodes and linkers allows for the incorporation of moieties of different size and charge that can play a critical role in structural arrangement and guest encapsulation.[2] The introduction of redox-active components into discrete supramolecular assemblies[3] provides access to additional properties such as redox-controlled guest-host interactions[4].

Metal complexes of salen-type ligands (Salen = N_2O_2 *bis*(*Schiff*-base)-*bis*(phenolate)) have the potential for redox activity at either the ligand or the metal center upon one-electron oxidation,[5] and tuning the electron-donating ability of salen ligands provides a mechanism to control electronic structure[5a] for reactivity[6] or materials applications.[7] Incorporating a functional group capable of secondary metal coordination at the *para*-position of the phenolate, presents an opportunity to employ salens as linkers in coordination-driven self-assembly. Salen complexes have been used in this context,[8] however, their redox properties in such structures remain unexplored. In this work we investigate the incorporation of a redox-active Ni salen into a discrete self-assembled supramolecular structure, the associated electronic structure and stability upon oxidation.

Linear rigid bis-pyridyl nickel salen metalloligand (**1**) was synthesized following previous reports.[9] Single crystals of **1** were isolated from dichloromethane and an X-ray structure is shown in Figure S1, affording a linear ditopic metalloligand of 19.4 Å in length, suitable for coordination-driven assembly. The synthesis of the self-assembled system **2** was achieved by reacting metalloligand **1** and $Pd(en)(NO_3)_2$ nodes followed by anion exchange with PF_6^- to ensure better solubility in organic solvents (Scheme 1). While such an association process often provides a mixture of triangle and square that exist in equilibrium,[10] the resulting ESI-FTICR mass spectrum unambiguously supports formation of the tetrameric self-assembly **2** (Figure 1), with characteristic multicharged peaks at m/z = 955.70 and 1323.93 corresponding to $[\mathbf{2} - 4(PF_6^-)]^{4+}$ and $[\mathbf{2} - 3(PF_6^-)]^{3+}$, respectively.

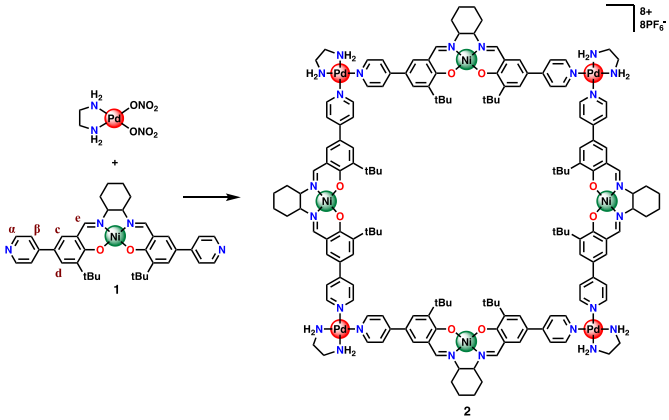

Scheme 1 Synthesis of **2**: (1) H_2O/THF, 295 K, 2h; (2) NH_4PF_6(aq), 295 K, 24h, 96% yield.

[a] Department of Chemistry, Simon Fraser University, Burnaby, Canada. E-mail: tim_storr@sfu.ca
[b] Laboratoire MOLTECH-Anjou, UMR CNRS 6200, UNIV Angers, SFR MATRIX, 2 Bd Lavoisier, 49045 Angers Cedex, France.

† Footnotes relating to the title and/or authors should appear here.
Electronic Supplementary Information (ESI) available: Detailed experimental section, crystallographic data for **1**, additional electrochemical and spectroscopic data (for **1** and **2**), and calculation details. See DOI: 10.1039/x0xx00000x

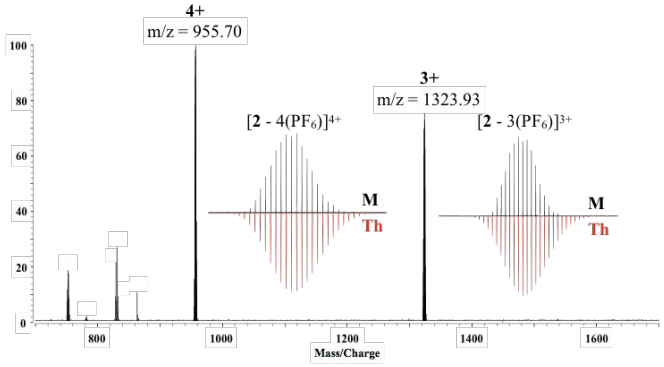

Figure 1 ESI-FTICR of **2** (10^{-3} M) in CH_3NO_2. Insets: experimental (M) and calculated (Th) isotopic pattern distribution of $[\mathbf{2}-4(PF_6)]^{4+}$ and $[\mathbf{2}-3(PF_6)]^{3+}$.

Coordination of the pyridyl groups to Pd(II) nuclei is further supported by a slight downfield shift of the Hα protons from 8.52 ppm in **1** to 8.60 ppm in **2**.[11] Additionally, ^{1}H DOSY NMR for **2** (see Figure 2 and ESI) showed a single set of signals with a diffusion rate of $D_{NMR} = 2.45 \times 10^{-10}$ m^2 s^{-1}, indicating that 1) only one discrete self-assembled structure exists in solution and 2) of a larger size in comparison to **1** ($D_{NMR} = 1.38 \times 10^{-9}$ m^2 s^{-1}). A Merck molecular force field (MMFF) calculation of **2** (Figure S2) predicts an outer and inner diameter of 37 Å and 20 Å, respectively. In addition, scanning transmission electron microscopy (STEM) measurements on **2** (see Figure S3) provide an average size of 32 ± 7 Å (see ESI for calculation details).

Cyclic voltammetry (CV) experiments reveal that complex **1** undergoes an irreversible oxidation at *ca.* 0.75 V vs. Fc^+/Fc (Figure 3a). This irreversibility is likely due to subsequent axial coordination of the pyridyl substituents of a separate Ni salen unit resulting in Ni(III) formation (*vide infra*).[12] Interestingly, coordination of metalloligand **1** to the Pd(II) nodes in self-assembly **2** precludes such an interaction and thus two quasi-reversible redox processes are observed at 0.78 V and 1.23 V (Figure 3b), illustrating the stability of square **2** during redox analysis. These redox potentials are comparable to a previously reported Ni salen complex containing a similar electron-withdrawing CF_3 functional group as the *para*-substituent.[13] To

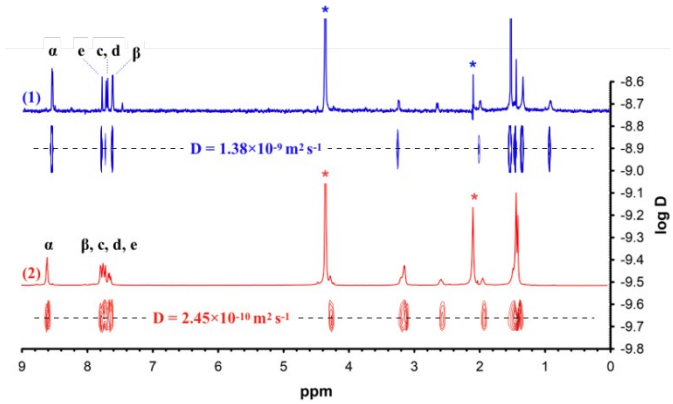

Figure 2 ^{1}H NMR with corresponding ^{1}H DOSY NMR of **1** (blue) and **2** (red) in CD_3NO_2. (*) Solvents: CH_3NO_2 (4.33 ppm) and H_2O (2.07 ppm).

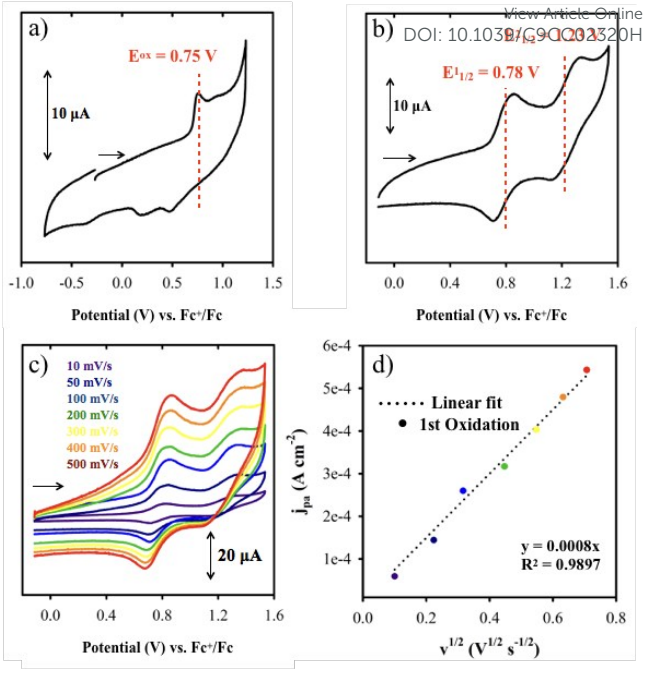

Figure 3 a) Cyclic voltammogram of **1** (0.50 mM, 100 mV s^{-1}); b) Cyclic voltammogram of **2** (0.25 mM, 100 mV s^{-1}); c) Potential scan rate dependence of **2** (0.25 mM) 10-500 mV s^{-1}; d) Linear regression between j_{pa} and the inverse scan rate of **2** at E^1_{ox}; Conditions: 0.1 M NBu_4PF_6 in CH_3NO_2 at 295 K.

further investigate the reversibility of the first oxidation, the Randles-Sevcik equation was used to estimate the diffusion coefficient from the electrochemical experiments (see ESI). Scan-rate dependence measurements (Figure 3c) were performed and the diffusion coefficient was calculated for the tetrameric assembly (n = 4 electrons) to be $D_{CV} = 2.22 \times 10^{-10}$ m^2 s^{-1} (Figure 3d), in excellent agreement with the above D_{NMR} value (D_{NMR}/D_{CV} for **2** is 1.10, which agrees with the published approximation of $D_{NMR} = 1.04 \times D_{CV}$).[14]

Oxidation of **1** with an aminium radical chemical oxidant, $[N(C_6H_3Br_2)_3]^{\bullet+}[SbF_6]^-$ ($E_{1/2}$ = 1.14 V vs. Fc^+/Fc)[15] was monitored *via* UV-Vis-NIR spectroscopy at low temperature in CH_3NO_2. The absorption spectrum of $[\mathbf{1}]^+$ remained featureless below 17,500 cm^{-1}, with an increase in absorption at *ca.* 23,000 cm^{-1} due to the amine oxidant by-product (Figure 4a).[13] The absence of absorption bands in the NIR is indicative of Ni(III) formation upon oxidation and was confirmed by EPR analysis (g_{avg} = 2.19, Figure S5).[16]

Table 1. Spectroscopic properties of $[\mathbf{2}]^{4\bullet+}$, $[\mathbf{fragment}]^{\bullet+}$ [a] and $[\mathbf{NiSal^{tBu}}]^{\bullet+}$ [b].

Complex	λ_{max} [cm^{-1}] (ε [M^{-1} cm^{-1}])	λ_{max} [cm^{-1}] (ε [M^{-1} cm^{-1}])
$[\mathbf{2}]^{4\bullet+}$	8,500 (48,100)	4,450 (94,700)
$[\mathbf{fragment}]^{\bullet+}$[a]	9,650 (f = 0.1247)	5,240 (f = 0.2318)
$[\mathbf{NiSal^{tBu}}]^{\bullet+}$[b]	9,200 (5,700)	4,700 (21,500)

[a]Molecular structure of the **fragment** (model compound) corresponds to metalloligand (**1**) coordinated to two Pd(II) nodes (see ESI for structure and calculation details); f – oscillator strength.
[b]Ref[17] (see Figure S4 for structure).

View Article Online
DOI: 10.1039/C9CC02320H

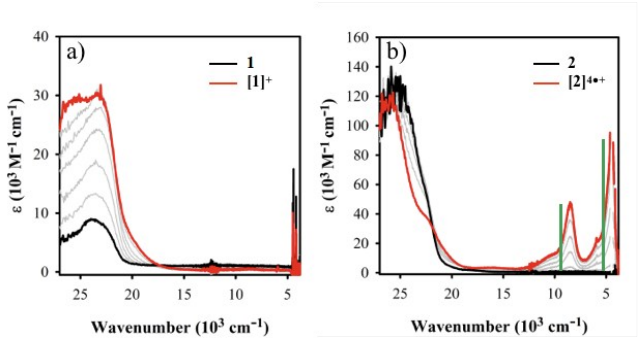

Figure 4 a) Electronic spectra of chemical oxidation of **1** (0.25 mM, black) to $[\mathbf{1}]^{+}$ (red); b) Electronic spectra of chemical oxidation of **2** (0.125 mM, black) to $[\mathbf{2}]^{4\bullet+}$ (red), TD-DFT predicted transitions for [**fragment**]$^{\bullet+}$ (green bars; see "a" in Table 1); Conditions: in CH_3NO_2, 253 K, titrated with 8 mM $[N(C_6H_3Br_2)_3]^{\bullet+}[SbF_6]^{-}$ as oxidant). Grey spectra represent aliquot additions of the oxidant. *Solvent peaks were removed for clarity (4130-4220 cm^{-1} and 4320-4615 cm^{-1}).

Oxidation of square **2** with $[N(C_6H_3Br_2)_3]^{\bullet+}[SbF_6]^{-}$ under the same conditions as the monomer (1 equiv. of oxidant per Ni center), afforded sharp and intense bands in the NIR region, at 8,500 cm^{-1} (ε = 48,100 M^{-1} cm^{-1}) and 4,450 cm^{-1} (ε = 94,700 M^{-1} cm^{-1}) (see Figure 4b). The extinction coefficient for the lowest energy band was estimated due to the overlap of solvent transitions in the region 4300-4600 cm^{-1} (see Figure S6 for the Gaussian fit of 4,450 cm^{-1} band). The energy and intensity of the low energy band agrees closely with the previously characterized ligand radical intervalence charge transfer (IVCT) band for $[NiSal^{tBu}]^{\bullet+}$ (*ca.* ¼ of intensity), which further supports ligand-based oxidation of the four metalloligands in $[\mathbf{2}]^{4\bullet+}$ (Table 1, Figure S4).[13,17] EPR analysis of $[\mathbf{2}]^{4\bullet+}$ in solution at 253 K is consistent with ligand radical formation, affording a broad isotropic signal at g_{avg} = 2.047 (Figure S7a). Interestingly, EPR analysis of $[\mathbf{2}]^{4+}$ at 100 K affords a Ni(III) signal (rhombic signal, g_{avg} = 2.172), consistent with a shift in the locus of oxidation from ligand to metal upon freezing (Figure S7b).[16] Complete disassembly of $[\mathbf{2}]^{4\bullet+}$ upon freezing is unlikely since the observed EPR spectra for $[\mathbf{1}]^{+}$ and $[\mathbf{2}]^{4+}$ at 100 K differ. We suggest that this result is due to axial ligation of a donor species to the Ni centers of the macrocycle, forming octahedral Ni(III) species at low temperature.[13] Similar temperature-dependent shifts in EPR signals have been observed for a number of monomeric Ni salen ligand radical systems upon freezing.[5d,13,17-18]

Due to the large size of square **2**, structural optimization and time-dependent density functional theory (TD-DFT) calculations were performed on a [**fragment**]$^{+}$, featuring complex **1** coordinated to two Pd(II) nodes (see Figure S8). As expected, the oxidized fragment is predicted to be a delocalized Ni salen ligand radical species with negligible spin density on the Pd nodes. In addition, the energies and relative intensities of the two low energy bands predicted by TD-DFT calculations (Table 1 and Figure S9) for the oxidized fragment are in close agreement with the experimental data for $[\mathbf{2}]^{4\bullet+}$. The donor (βHOMO) and acceptor (βLUMO) orbitals attributed to the predicted low energy NIR transition are delocalized over the salen ligand, consistent with assignment as a ligand radical IVCT transition.[17,19] The combination of the experimental data and calculations thus support ligand-based oxidation of each of the Ni salen units of **2** to form $[\mathbf{2}]^{4\bullet+}$.

Finally, the stability of $[\mathbf{2}]^{4\bullet+}$ and the reversibility of the oxidation was investigated *in situ* at 253 K, by monitoring the absorption band at 8,500 cm^{-1}. After 15 hours, only *ca.* 30% of the oxidized species had decayed (Figure S10). In addition, $[\mathbf{2}]^{4\bullet+}$ could be reduced to **2** with four equivalents of decamethylferrocene ($FeCp^*_2$), and then re-oxidized to $[\mathbf{2}]^{4\bullet+}$ with an additional four equivalents of oxidant, resulting in minimal decomposition of the macrocycle (Figure S11).

In conclusion, we report a route to coordination-driven assembly of a square macrocycle **2**, incorporating four redox-active salen ligands. While oxidation of Ni salen complex **1** affords a Ni(III) species, controlled oxidation of square **2** results in ligand radical formation of each of the four Ni salen units, thus highlighting the change in oxidation locus upon coordination-driven assembly. The application of supramolecular assemblies containing salen ligand radical units for redox-controlled guest-host interactions is now being explored.

Conflicts of interest

There are no conflicts to declare.

Acknowledgments

This work was supported by a Natural Sciences and Engineering Research Council (NSERC) Discovery Grant (RGPIN-2014-05240 T. S.). K. H. thanks Mitacs Canada for a Globalink Fellowship. The authors gratefully acknowledge Prof. Charles Walsby for access to EPR instrumentation. The authors are also thankful to Prof. Frédéric Aubriet and Dr. Vincent Carré, Univ. Lorraine, for ESI-FTICR mass spectrometry measurements and Dr. Eric Ye, Simon Fraser University, for his assistance with DOSY NMR spectroscopy. Compute Canada is thanked for access to computational resources.

Notes and references

1. (a) S. Datta, M. L. Saha and P. J. Stang, *Acc. Chem. Res.*, 2018, **51**, 2047-2063; (b) Y. Lu, H. N. Zhang and G. X. Jin, *Acc. Chem. Res.*, 2018, **51**, 2148-2158; (c) A. Casini, B. Woods and M. Wenzel, *Inorg. Chem.*, 2017, **56**, 14715-14729; (d) T. R. Cook and P. J. Stang, *Chem. Rev.*, 2015, **115**, 7001-7045; (e) A. J. McConnell, C. S. Wood, P. P. Neelakandan and J. R. Nitschke, *Chem. Rev.*, 2015, **115**, 7729-7793; (f) K. Harris, D. Fujita and M. Fujita, *Chem. Commun.*, 2013, **49**, 6703-6712; (g) R. Chakrabarty, P. S. Mukherjee and P. J. Stang, *Chem. Rev.*, 2011, **111**, 6810-6918.
2. (a) S.-L. Huang, T. S. A. Hor and G.-X. Jin, *Coord. Chem. Rev.*, 2017, **333**, 1-26; (b) B. Roy, R. Saha, A. K. Ghosh, Y. Patil and P. S. Mukherjee, *Inorg. Chem.*, 2017, **56**, 3579-3588; (c) S. Wang, T. Sawada and M. Fujita, *Chem. Commun.*, 2016, **52**, 11653-11656; (d) W. Wang, Y. X. Wang and H. B. Yang, *Chem. Soc. Rev.*, 2016, **45**, 2656-2693; (e) S. Bivaud, J. Y. Balandier, M. Chas, M. Allain, S. Goeb and M. Salle, *J. Am. Chem. Soc.*, 2012, **134**, 11968-11970.

3. (a) R. F. Winter, *Curr. Opin. Electrochem.*, 2018, **8**, 14-23; (b) V. Croue, S. Goeb and M. Salle, *Chem. Commun.*, 2015, **51**, 7275-7289; (c) L. Xu, Y. X. Wang, L. J. Chen and H. B. Yang, *Chem. Soc. Rev.*, 2015, **44**, 2148-2167.
4. (a) T. Y. Kim, R. A. S. Vasdev, D. Preston and J. D. Crowley, *Chem. Eur. J.*, 2018, **24**, 14878-14890; (b) G. Szaloki, V. Croue, V. Carre, F. Aubriet, O. Aleveque, E. Levillain, M. Allain, J. Arago, E. Orti, S. Goeb and M. Salle, *Angew. Chem. Int. Ed.*, 2017, **56**, 16272-16276; (c) V. Croue, S. Goeb, G. Szaloki, M. Allain and M. Salle, *Angew. Chem. Int. Ed.*, 2016, **55**, 1746-1750.
5. (a) R. M. Clarke, K. Herasymchuk and T. Storr, *Coord. Chem. Rev.*, 2017, **352**, 67-82; (b) F. Thomas, *Dalton Trans.*, 2016, **45**, 10866-10877; (c) C. T. Lyons and T. D. Stack, *Coord. Chem. Rev.*, 2013, **257**, 528-540; (d) Y. Shimazaki, F. Tani, K. Fukui, Y. Naruta and O. Yamauchi, *J. Am. Chem. Soc.*, 2003, **125**, 10512-10513.
6. (a) R. M. Clarke and T. Storr, *J. Am. Chem. Soc.*, 2016, **138**, 15299-15302; (b) L. Chiang, L. E. Allan, J. Alcantara, M. C. Wang, T. Storr and M. P. Shaver, *Dalton Trans.*, 2014, **43**, 4295-4304; (c) D. J. Darensbourg, R. M. Mackiewicz, A. L. Phelps and D. R. Billodeaux, *Acc. Chem. Res.*, 2004, **37**, 836-844; (d) E. N. Jacobsen, W. Zhang and M. L. Guler, *J. Am. Chem. Soc.*, 1991, **113**, 6703-6704.
7. (a) R. M. Clarke, T. Jeen, S. Rigo, J. R. Thompson, L. G. Kaake, F. Thomas and T. Storr, *Chem. Sci.*, 2018, **9**, 1610-1620; (b) H. Houjou, M. Ito and K. Araki, *Inorg. Chem.*, 2011, **50**, 5298-5306; (c) T. Glaser, M. Heidemeier, T. Weyhermuller, R. D. Hoffmann, H. Rupp and P. Muller, *Angew. Chem. Int. Ed.*, 2006, **45**, 6033-6037.
8. (a) Y. M. Jeon, J. Heo and C. A. Mirkin, *J. Am. Chem. Soc.*, 2007, **129**, 7480-7481; (b) M. S. Masar, 3rd, N. C. Gianneschi, C. G. Oliveri, C. L. Stern, S. T. Nguyen and C. A. Mirkin, *J. Am. Chem. Soc.*, 2007, **129**, 10149-10158; (c) S. S. Sun, C. L. Stern, S. T. Nguyen and J. T. Hupp, *J. Am. Chem. Soc.*, 2004, **126**, 6314-6326.
9. (a) K. Senthil Murugan, T. Rajendran, G. Balakrishnan, M. Ganesan, V. K. Sivasubramanian, J. Sankar, A. Ilangovan, P. Ramamurthy and S. Rajagopal, *J. Phys. Chem. A*, 2014, **118**, 4451-4463; (b) W.-S. Kim, K. Y. Lee, E.-H. Ryu, J.-M. Gu, Y. Kim, S. J. Lee and S. Huh, *Eur. J. Inorg. Chem.*, 2013, 4228-4233; (c) G. A. Morris, H. Zhou, C. L. Stern and S. T. Nguyen, *Inorg. Chem.*, 2001, **40**, 3222-3227.
10. (a) M. Ferrer, A. Pedrosa, L. Rodriguez, O. Rossell and M. Vilaseca, *Inorg. Chem.*, 2010, **49**, 9438-9449; (b) T. Weilandt, R. W. Troff, H. Saxell, K. Rissanen and C. A. Schalley, *Inorg. Chem.*, 2008, **47**, 7588-7598.
11. M. Agnes, A. Nitti, D. A. Vander Griend, D. Dondi, D. Merli and D. Pasini, *Chem. Commun.*, 2016, **52**, 11492-11495.
12. Electrochemistry experiments of Ni salen complexes in the presence of excess pyridine exhibit irreversibility due to oxidation followed by subsequent axial pyridine binding to form an octahedral d7 Ni(III) complex. See Figure S4.
13. L. Chiang, K. Herasymchuk, F. Thomas and T. Storr, *Inorg. Chem.*, 2015, **54**, 5970-5980.
14. H. Sun, W. Chen and A. E. Kaifer, *Organometallics*, 2006, **25**, 1828-1830.
15. N. G. Connelly and W. E. Geiger, *Chem. Rev.*, 1996, **96**, 877-910.
16. (a) M. Eckshtain-Levi, M. Orio, R. Lavi and L. Benisvy, *Dalton Trans.*, 2013, **42**, 13323-13326; (b) D. Pinho, P. Gomes, C. Freire and B. de Castro, *Eur. J. Inorg. Chem.*, 2001, 1483-1493; (c) S. A. Jacobs and D. W. Margerum, *Inorg. Chem.*, 1984, **23**, 1195-1201; (d) A. Bencini, L. Fabbrizzi and A. Poggi, *Inorg. Chem.*, 1981, **20**, 2544-2549.
17. T. Storr, E. C. Wasinger, R. C. Pratt and T. D. P. Stack, *Angew. Chem.*, 2007, **119**, 5290-5293.
18. (a) L. Benisvy, R. Kannappan, Y.-F. Song, S. Milikisyants, M. Huber, I. Mutikainen, U. Turpeinen, P. Gamez, L. Bernasconi, E. J. Baerends, F. Hartl and J. Reedijk, *Eur. J. Inorg. Chem.*, 2007, **2007**, 637-642; (b) Y. Shimazaki, T. Yajima, F. Tani, S. Karasawa, K. Fukui, Y. Naruta and O. Yamauchi, *J. Am. Chem. Soc.*, 2007, **129**, 2559-2568; (c) O. Rotthaus, O. Jarjayes, F. Thomas, C. Philouze, C. P. Del Valle, E. Saint-Aman and J. L. Pierre, *Chem. Eur. J.*, 2006, **12**, 2293-2302.
19. (a) N. M. Mews, A. Berkefeld, G. Horner and H. Schubert, *J. Am. Chem. Soc.*, 2017, **139**, 2808-2815; (b) D. M. D'Alessandro and F. R. Keene, *Chem. Soc. Rev.*, 2006, **35**, 424-440.

View Article Online
DOI: 10.1039/C9CC02320H